Wi-Fi Multi-Path Parameter Estimation for Sub-7 GHz Sensing: A Comparative Study

Francesca Meneghello*, Alejandro Blanco§, Antonio Cusano*, Joerg Widmer†, Michele Rossi*‡
* Department of Information Engineering, University of Padova, Italy
§ School of Informatics, The University of Edinburgh, United Kingdom
† IMDEA Networks Institute, Madrid, Spain
‡ Department of Mathematics "Tullio Levi-Civita", University of Padova, Italy
e-mail: francesca.meneghello.1@unipd.it, alejandro.blanco@ed.ac.uk, antonio.i.cusano@gmail.com,
joerg.widmer@imdea.org, michele.rossi@unipd.it

***Abstract*—Thanks to the definition of the new IEEE 802.11bf standard, the development of Wi-Fi sensing applications is gaining momentum in the research community. In this regard, several studies have shown that learning-based approaches that leverage the frequency response of the Wi-Fi channel in the sub-7 GHz bands can reach high accuracy in different classification tasks, such as activity recognition, or person identification. Instead, more fine-grained applications – e.g., human localization and tracking, or respiration and heartbeat monitoring – require implementing model-based approaches to estimate the Wi-Fi multi-path parameters and analyze the time evolution of the paths associated with specific targets (the human body or chest). In this paper, we investigate the performance of six super-resolution algorithms for sub-7 GHz multi-path parameter estimation. Our extensive evaluation indicates that the estimation accuracy that can be achieved through commercial devices allows implementing human localization and tracking strategies but is insufficient to effectively design human vital signs monitoring applications due to the limited frequency and spatial diversity. We pledge to release our implementations for further investigations.[1]**

***Index Terms*—Wi-Fi sensing, multi-path, CFR, IEEE 802.11.**

I. Introduction

Wireless sensing through commercial Wi-Fi devices has been extensively studied in recent years, leading to the development of several applications, among which active and passive localization, vital sign monitoring, and activity/gesture recognition [1]. The main intuition behind Wi-Fi sensing is to study the multi-path signal propagation to obtain information about static and moving targets that irradiate radio waves (active sensing) or act as signals reflectors, diffractors or scatterers (passive sensing). In turn, the Wi-Fi channel state information (CSI) has been extensively leveraged by researchers over the last decade for active and passive contactless sensing.

A key advantage of Wi-Fi-based systems with respect to systems based on cameras or radar is that they allow reusing devices already deployed for communication purposes without the burden of installing additional hardware. This aroused the interest of the industrial community that is currently working on the standardization of a new amendment to the IEEE 802.11 Wi-Fi standard, named IEEE 802.11bf, that will enable the joint provisioning of the communication and the sensing services [2]. IEEE 802.11bf will enable sensing in both the sub-7 GHz and the millimeter wave (mmWave) spectrum (60 GHz bands) by properly modifying the physical and medium access control layers of the Wi-Fi protocol stack [3]. The choice of the sensing frequency band depends on the sensing scenario and the required sensing accuracy since the wireless channel at sub-7 GHz and mmWave frequencies have different radio wave propagation characteristics. On the one hand, sub-7 GHz frequencies allow implementing sensing applications that require a through-the-wall view or the collection of a huge number of multi-path components. This is not possible on the 60 GHz spectrum as the propagation of a mmWave signal is completely blocked by obstacles in the environment and the mmWave channel is much more sparse than the sub-7 GHz channels. On the other hand, mmWave bands enable a higher sensing granularity given the higher available bandwidth.

In this paper, we focus on passive Wi-Fi sensing on the sub-7 GHz bands – as they are currently supported by commercial Wi-Fi devices on the market. Several learning-based and model-based algorithms have been proposed over the year to properly leverage the Wi-Fi CSI for different applications. Learning-based algorithms are used when a coarse estimation of the variability in the propagation environment is sufficient to associate the CSI traces to specific classes of situations. Examples of applications enabled by this approach are person identification [4], and human activity recognition [5]. Model-based algorithms are instead adopted when an accurate estimation of the multi-path propagation is needed, e.g., for localization and tracking [6]. In this respect, multi-path profiling algorithms have been developed to estimate the parameters of the multi-path components and obtain information about the single objects in the environment acting as reflectors/diffractors/scatterers for the Wi-Fi signal [6]. Localization approaches infer the physical position of the target from the multi-path estimation. Hence, tracking is performed by associating the estimates over subsequent time instants by proximity. In this paper, we aim at understanding whether multi-path parameter estimation approaches can be leveraged for more fine-grained applications such as respiration and heartbeat monitoring. The challenge is that, differently from tracking, the association should be performed directly on the multi-path components instead that on the inferred physical position. This would enable implementing radar-like applications that obtain the vital sign traces by collecting the phase of a single multi-path component in time [7]. Existing approaches for Wi-Fi-based vital sign monitoring rely on the analysis of the complete CSI and thus require the users to remain still during the experiment [1]. Considering a single multi-path component would instead allow compensating for small human movements. We

[1] https://github.com/francescamen/Wi-Fi-multipath-parameter-estimation

conduct a comparative analysis considering three approaches from the literature, i.e., mD-Track [6], SpotFi [8] and UbiLocate [9], together with three other approaches we designed and implemented for this task based on compressive sensing. The analysis is performed by simulating the Wi-Fi channel for a single transmission link, by changing the respective positions (distance and orientation) of the transmitter and the receiver. The results show that even using recent super-resolution multi-path parameter estimators, the achievable estimation accuracy is not sufficient to effectively develop vital signs monitoring applications based on single multi-path components. Overall, our evaluation provides a clear view of the limits of sub-7 GHz Wi-Fi sensing, providing other researchers with useful hints for the development of new passive sensing applications to be integrated into next-generation IEEE802.11bf Wi-Fi networks.

II. Wi-Fi Multi-Path Channel Model

We consider a single-input, multi-output (SIMO) system where the transmitter has a single antenna and the receiver has a uniform linear array of N antennas spaced apart by half of the carrier wavelength. The extension to the case of a multi-input, multi-output (MIMO) system can be done by considering multiple SIMO systems, one for each transmitting antenna. Wi-Fi devices operating on the sub-7 GHz bands, i.e., following the IEEE 802.11n/ac/ax standards, leverage the orthogonal frequency-division multiplexing (OFDM) or orthogonal frequency-division multiple access (OFDMA) modulation schemes to transmit the signal over K partially overlapping sub-channels with center frequencies spaced apart by Δ_f. The signal propagates through the radio channel following P different paths (multi-path propagation phenomenon) that combine at the receiver device, as depicted in Fig. 1. Each path is characterized by a signal amplitude attenuation γ_p, an angle of arrival (AoA) at the receiver $\theta_{\text{rx},p}$, and a propagation delay (or time of arrival (ToA) at the receiver) τ_p with $P \in \{0, P-1\}$. The way the different components combine in the signal measured at the receiver is described next [10].

Propagation delay (or ToA) τ_p. The propagation delay depends on the path length and reflects, in the frequency domain, in a phase shift $[\psi(\tau_p)]_k$ for each OFDM sub-channel k, expressed as

$$[\psi(\tau_p)]_k = e^{-j2\pi k \Delta_f \tau_p} . \tag{1}$$

Angle of arrival (AoA) $\theta_{\text{rx},p}$. The AoA introduce a phase shift ($[\phi(\theta_{\text{rx},p})]_n$) in the frequency domain between signals collected by each different receiving antenna n. Specifically, assuming that the antenna spacing is half of a carrier wavelength, the phase shift for the p^{th} path is given by

$$[\phi(\theta_{\text{rx},p})]_n = e^{-j\pi n \sin(\theta_{\text{rx},p})} . \tag{2}$$

Multi-path signal. Considering all the K OFDM sub-channels and the N receiving antennas, the vectors collecting the phase shifts associated with the ToA and AoA are respectively

$$\boldsymbol{\psi}(\tau_p) = \left[[\psi(\theta_p)]_0, ..., [\psi(\tau_p)]_{K-1}\right] , \text{and} \tag{3}$$

$$\boldsymbol{\phi}(\theta_{\text{rx},p}) = \left[[\phi(\theta_{\text{rx},p})]_0, ..., [\phi(\theta_{\text{rx},p})]_{N-1}\right] . \tag{4}$$

Hence, being $\mathbf{s}$ the frequency domain representation of the transmitted signal, and $\mathbf{w}$ white Gaussian noise, the received signal is obtained (in the frequency domain) as $\mathbf{y} = \mathbf{H}\mathbf{s} + \mathbf{w}$ where $\mathbf{H}$ is the $N \times K$-dimensional channel frequency response (CFR) matrix. Considering the above contributions to the phase shift of the collected signal, $\mathbf{H}$ is formulated as

$$\mathbf{H} = \sum_{p=0}^{P-1} \gamma_p \boldsymbol{\phi}(\theta_{\text{rx},p}) \boldsymbol{\psi}(\tau_p) . \tag{5}$$

The time domain representation of the CFR is referred to as channel impulse response (CIR) and is indicated as $\mathbf{h}$ in the following. The CIR is the combination of P impulses each characterized by amplitude γ_p, ToA τ_p and AoA $\theta_{\text{rx},p}$.

A. Channel Frequency Response-based Wi-Fi Sensing

The CFR is the most widely used data for sensing as it contains individual channel contributions of different objects in the environment and provides frequency and spatial diversity. The vast majority of the sensing approaches in the literature obtain information about the environment by analyzing small perturbations in the CFR caused by the changes in the multi-path propagation. This approach allows designing *qualitative* learning-based methods that recognize human activities, hand gestures, and person identities, among others [1]. The design of Wi-Fi sensing applications that require *quantitative* estimation of the Wi-Fi channel is instead more challenging. Examples of such applications are passive person localization and tracking, and human vital signs monitoring. These applications require obtaining precise information about the multi-path associated with the reflecting/diffracting/scattering objects in the environment to track their changes in time. To this end, the parameters of the multi-path components need to be estimated based on the CFR matrix collected at the sensing station in order to separate the contribution of every obstacle.

B. Challenges of Path Parameter Estimation at sub-7 GHz.

The most straightforward approach to obtain the CIR $\mathbf{h}$ is by computing the inverse discrete Fourier transform (IDFT) of the CFR $\mathbf{H}$ over the OFDM sub-channels and the receiving antennas dimensions. Using this approach, the accuracy in the multi-path parameter estimation is constrained by the CFR diversity in the frequency and spatial domains. Specifically, the ToA nominal resolution $\Delta\tau_p$ is linked with the available bandwidth B as $\Delta\tau_p = 1/B$, and the AoA nominal resolution

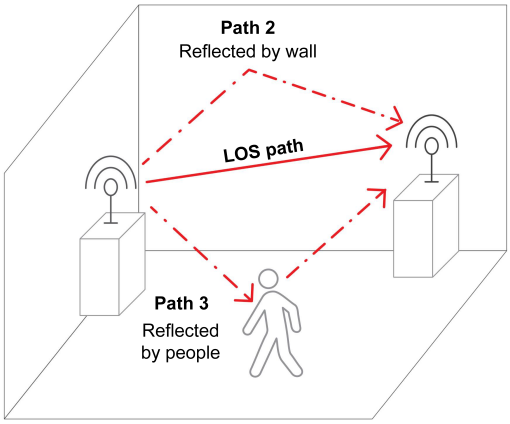

Fig. 1: Multi-path propagation of a Wi-Fi signal through three paths: the line of sight (LoS) and two reflected paths.

is associated with the number of monitoring antennas N as $\Delta\theta_{\mathrm{rx},p} = 360/(\pi N)$ degrees. Current IEEE 802.11 devices offer up to a maximum of $160\,\mathrm{MHz}$ of bandwidth and, in turn, the nominal resolution is about $6\,\mathrm{ns}$ meaning that paths with a length difference smaller than 1.8 meters cannot be properly separated. Moreover, the number of antennas available in commercial Wi-Fi devices is limited to 4 for each band thus providing low spatial diversity. Super-resolution algorithms can be used to deal with these limitations and obtain more precise estimates by leveraging the sparse nature of the Wi-Fi channel in the ToA and AoA domains as discussed next.

III. Wi-Fi Multi-Path Parameter Estimation: Problem Formulation

Based on the sparse nature of the Wi-Fi channel, the multi-path parameter estimation can be formulated as a *sparse recovery* problem as it entails obtaining a sparse vector $\mathbf{h}$ – representing the CIR – by leveraging the multi-path propagation information in the CFR. In the following, $\mathbf{h}$ is a P'-dimensional vector, where P' represents the number of candidate multi-path components specified by specific ToA and AoA. Among these, only the $P < P'$ components associated with reflectors/diffractors/scatterers in the environment are different from zero. The sparse recovery problem is formulated as a constrained minimization of the L^0-norm of $\mathbf{h}$ as

$$\mathbf{P1}: \quad \mathbf{h} = \underset{\tilde{\mathbf{h}}}{\operatorname{argmin}} \ \|\tilde{\mathbf{h}}\|_0, \quad \text{subject to} \ \ \mathbf{H} = \mathbf{T}\tilde{\mathbf{h}} \tag{6}$$

where $\mathbf{T}$ is a $(K \times N) \times P'$ matrix describing how the P' candidate paths combine at each of the K OFDM sub-channels and N receiving antennas. The matrix $\mathbf{T}$ is user-defined and depends on the selected ToA and AoA granularity. When dealing with noisy data, the equality constraint in Eq. (6) has to be relaxed to an inequality one as $\|\mathbf{H} - \mathbf{T}\tilde{\mathbf{h}}\|_2^2 < \epsilon$ where $\epsilon > 0$ is the parameter defining the tolerable error. Hence, P1 can be reformulated as

$$\mathbf{P2}: \quad \mathbf{h} = \underset{\tilde{\mathbf{h}}}{\operatorname{argmin}} \ \|\mathbf{H} - \mathbf{T}\tilde{\mathbf{h}}\|_2^2, \tag{7}$$

$$\text{subject to} \ \ \|\tilde{\mathbf{h}}\|_0 < m\,, \tag{8}$$

where m is the (user-defined) number of non-zero components of the sparse vector $\tilde{\mathbf{h}}$, i.e., the number of elements in the support set of $\tilde{\mathbf{h}}$.

In the following, we present and analyze the performance of six multi-path parameter estimation algorithms based on sparse recovery investigating the trade-off between accuracy and complexity. Three of the considered approaches are specifically designed for this purpose and are presented in Section IV. The remaining three are instead based on two compressive sensing reconstruction strategies and are detailed in Section V.

IV. Ad-Hoc Approaches for Wi-Fi Multi-Path Parameter Estimation

Here we present SpotFi, mD-Track and UbiLocate, being three state-of-the-art approaches for Wi-Fi multi-path parameter estimation, respectively presented in [8], [6], and [9].

SpotFi approach. SpotFi is an active Wi-Fi localization system proposed in [8]. The algorithm is based on the joint angle and delay estimation (JADE) algorithm. JADE was proposed in [11] as an extension of the multiple signal classification (MUSIC) algorithm in [12] for concurrently estimating the ToA and AoA parameters. JADE estimates the $\mathbf{h}$ matrix through the following steps. First, the CFR $\mathbf{H}$ is decomposed through eigendecomposition. Hence, the eigenvectors are grouped into a signal and a noise sub-space. The signal sub-space contains the eigenvectors representing the incident signal, i.e., associated with eigenvalues higher than a certain user-defined threshold. The remaining eigenvectors define the noise sub-space and their concatenation into a matrix is here referred to as $\mathbf{E}$. From the orthogonality of the eigenvectors, it follows that the signal and the noise sub-spaces are orthogonal. In turn, being $\mathbf{T}(\tau, \theta_{\mathrm{rx}})$ the element of the matrix $\mathbf{T}$ associated with ToA τ and AoA θ_{rx}, the P peaks in the $S(\tau, \theta_{\mathrm{rx}})$ spectrum defined as

$$S(\tau, \theta_{\mathrm{rx}}) = \frac{1}{\mathbf{T}^\dagger(\tau, \theta_{\mathrm{rx}})\mathbf{E}\mathbf{E}^\dagger\mathbf{T}(\tau, \theta_{\mathrm{rx}})}\,, \tag{9}$$

provide the estimates of the signal multi-path parameters τ_p and $\theta_{\mathrm{rx},p}$ for $p \in \{0, P-1\}$. The $\dagger$ symbol in Eq. (9) indicates the hermitian operator.

mD-Track approach. mD-Track is a Wi-Fi passive localization system that can jointly estimate the angle of arrival and departure, the path delay and the Doppler parameters of the multi-path components of the signal [6]. To compare mD-Track with the other approaches, in this paper we consider the two-dimensional version of the algorithm that estimates the ToA and AoA parameters based on two phases. The first phase consists in obtaining a coarse estimation of the parameters of the multi-path signal by iteratively estimating the strongest multi-path component and removing it from the signal by signal subtraction. During this phase, mD-Track also obtains an estimate of the background noise. The second phase is a refinement step built upon the space-alternating generalized expectation maximization (SAGE) iterative algorithm [13]. The SAGE algorithm splits the estimation of the parameters of the multi-path components into multiple estimates of the parameters of a single component. Specifically, in mD-Track, the process proceeds iteratively by re-estimating every single path found in the preliminary phase by continuously updating the background noise estimate. In each of the two phases, the mD-Track algorithm finds the strongest path at each iteration by solving problem P2 in Eq. (7) setting $m = 1$, i.e., $\mathbf{h}$ has only one non-zero component which value indicates the amplitude of the multi-path component while the position in the $P' \times 1$ dimensional vector indicates the path ToA and AoA.

UbiLocate approach. UbiLocate is an active Wi-Fi-based localization system proposed in [9]. The algorithm is designed to provide high accuracy in non line of sight (NLoS) settings. To do so, UbiLocate proposes a high-resolvability multi-path parameter estimation algorithm based on two steps. In the first step, UbiLocate performs a greedy matching projection to iteratively estimate the multi-path parameters following the same general idea of mD-Track. Specifically, $\mathbf{h}$ is obtained from $\mathbf{H}$ through an oversampled inverse discrete Fourier transform, i.e., $\mathbf{T}$, in this case, represents the matrix of the Fourier

transformation. The strongest component in the resulting $\mathbf{h}$ is hence removed from $\mathbf{H}$ and the process iterates to find the estimate of all the multi-path components in the signal. In the second phase, UbiLocate performs a refinement of the estimates through a Nelder-Mead search that minimizes Eq. (7) starting from the estimates obtained through the first phase.

V. Compressive Sensing Reconstruction-based Approaches for Multi-Path parameter Estimation

The use of *compressive sensing reconstruction* algorithms for multi-path parameter estimation was first analyzed in [14], [15]. Here we focus on three greedy algorithms that solve the approximate minimization problem P2. Greedy algorithms proceed iteratively making local optimal choices and are categorized into *greedy pursuit* and *thresholding*-based. Next we present and evaluate the orthogonal matching pursuit (OMP) and the iterative hard thresholding (IHT) methods, that respectively belong to the former and latter classes [16].

Orthogonal Matching Pursuit (OMP). Greedy pursuit algorithms generate an estimate of $\mathbf{h}$ starting from a zero vector and iteratively adding new components whose value is optimized based on the minimization of the cost function in Eq. (7) [16]. Specifically, at each iteration, OMP finds the column of $\mathbf{T}$ most correlated with the current residual and adds it to a set denoted as active columns. Then, it estimates a solution to Eq. (7) through the least squares method restricted to the active columns only. The process is iterated until the residual, i.e., $\|\mathbf{H} - \mathbf{T}\tilde{\mathbf{h}}\|_2^2$ is smaller than a threshold.

Iterative Hard Thresholding (IHT). Thresholding methods first find an $\mathbf{h}$ that minimizes the cost function and hence prune it based on thresholding strategies that maintain only the m most significant elements of $\mathbf{h}$ [16]. Based on this general idea, IHT iterates by updating a candidate solution $\tilde{\mathbf{h}}$ following the direction of decreasing gradient of the reconstruction error $\|\mathbf{H} - \mathbf{T}\tilde{\mathbf{h}}\|_2^2$. Specifically, the gradient is obtained as $\mathbf{g} = \mathbf{T}^T(\mathbf{H} - \mathbf{T}\tilde{\mathbf{h}})$ – where T is the transpose operator – and an update coefficient $\mu > 0$ is defined to implement the update. After every update, a nonlinear projection (called thresholding function) is applied to the candidate solution to approximate it with its m most significant terms while setting the remaining elements to zero. To maximally reduce the reconstruction error at each iteration, μ is optimally selected based on the value of the gradient. The process continues until the difference between the $\tilde{\mathbf{h}}$ estimated in two consecutive iterations becomes smaller than a certain threshold. For the purpose of Wi-Fi multi-path parameter estimation, we designed a customized thresholding function that considers the physical meaning of the elements in $\mathbf{h}$, i.e., the Wi-Fi propagation paths. Specifically, we selected the entries to be retained through the thresholding function by performing a peak search in the candidate $\tilde{\mathbf{h}}$ signal and retaining the elements associated with the stronger peaks. This allows forcing a lower bound regarding the distance between the selected elements thus obtaining a solution for $\mathbf{h}$ in line with its physical interpretation.

Wi-Fi multi-path parameters	
ToA first path	1×10^{-8} s
ToA second path	$\in [1.02, \ldots, 2] \times 10^{-8}$ s
ToA step	2×10^{-10} s
AoA first path	$\in [-90, \ldots, 90]$ deg
AoA second path	$\in [-90, \ldots, 90]$ deg
AoA step	1 deg 1^{st} - 2 deg 2^{nd}

TABLE I: Multi-path propagation parameters.

Iterative Hard Thresholding (IHT) with Refinement. As another solution to perform parameter estimation, we implemented IHT including an additional iterative refinement step that takes inspiration from the mD-Track approach. The process starts by detecting the most powerful path in $\tilde{\mathbf{h}}$, and reconstructing and removing it from $\mathbf{H}$. Next, the IHT algorithm presented above is executed again to obtain a new estimate of $\mathbf{h}$. Hence, the strongest path in the new $\tilde{\mathbf{h}}$ is extracted and removed from $\mathbf{H}$ and the process continues until the power of the detected strongest path is below a threshold.

VI. Numerical Results and Comparison

To quantitatively evaluate and compare the performance of the six approaches for multi-path parameter estimation described above, we simulated a Wi-Fi channel with a two-ray model, where the first path is the LoS while the second represents a reflected/diffracted/scattered signal from an object in the environment. Each ray is characterized by a propagation delay (ToA), an AoA at the receiver, and a unitary amplitude as described in Section II. Note that previous evaluations in the literature, e.g., [6], only considered a fixed value for the AoA of the LoS signal. This limits a thorough evaluation of the approaches as they only consider a specific respective orientation of the transmitter and receiver antenna arrays. In this work, we deepen the analysis by considering different values for the LoS AoA, thus representing different orientations of the antenna arrays at the transmitting and the receiving Wi-Fi devices. To do that, we changed the AoA of the LoS from -90 deg to 90 deg in our evaluations. Hence, several ToA/AoA combinations have been considered for the second path, as summarized in Table I. In the following, we present the results obtained when using the algorithms described in Sections IV-V to estimate the multi-path parameters in the signal. Specifically, we want to understand the minimum ToA and AoA differences that two paths should have in order to be properly recognized as two distinct contributions to the CFR – i.e., be *resolvable* – and associated with accurate estimates for the ToA and AoA. The resolvability, and ToA and AoA error heatmaps presented next have been obtained by averaging the results over all the simulations for the same ToA and AoA difference between the two paths obtaining 91 different terms for each average. For the execution time, the average is computed considering all the $823\,550$ simulations obtained for each setting, i.e., (181 AoA for the 1^{st} path) $\times$ (91 AoA for the 2^{nd} path) $\times$ (50 ToA for the 2^{nd} path) (see Table II). The algorithms have been executed on an Intel™ Xeon™ Gold 5118 CPU in single threads using eight cores each.[2]

[2]The code of the implementations is available at https://github.com/francescamen/Wi-Fi-multipath-parameter-estimation

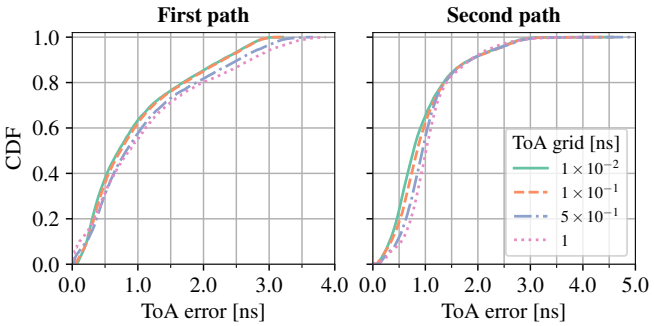

Fig. 2: mD-Track ToA estimation error for the first (left) and the second (right) paths changing the ToA grid granularity.

ToA grid [ns]	time [$\times 10^{-2}$ s]
1×10^{-2}	15.2
1.0×10^{-1}	2.1
5.0×10^{-1}	1.2
1.00	0.9

method	time [$\times 10^{-2}$ s]
mD-Track	1.2
SpotFi	72.9
UbiLocate	2.3
IHT	113.8
IHT enhanced	140.3
OMP	235.9

TABLE II: Average execution time for the multi-path parameter estimators in Sections IV-V. The execution time of mD-Track varying the ToA grid granularity is on the left.

Hyper-parameters selection. The multi-path parameter estimation approaches rely on a matrix of candidate paths, referred to as $\mathbf{T}$ in Section III. Such $\mathbf{T}$ matrix is defined through a set of candidate ToA and AoA which combinations generate the P' candidate paths following Eq. (5). Ideally, P' should contain an infinite number of candidate paths to properly estimate the multi-path parameters. However, this would imply performing matrix multiplications with huge matrices that would be computationally prohibitive. Moreover, even if the super-resolution algorithms described above can increase the ToA and AoA resolutions, the physical limitations linked with the bandwidth and the number of antennas do not allow increasing it indefinitely with respect to the nominal resolution (see Section II-B). In turn, the grid granularity needs to be properly selected. In Fig. 2 we evaluate how the ToA grid granularity affects the performance of the mD-Track path parameter estimator. We fix the AoA grid granularity to 0.5 deg and change the grid for the ToA in $\{1 \times 10^{-11}, 1 \times 10^{-10}, 5 \times 10^{-10}, 1 \times 10^{-9}\}$ s. The computation time for the estimation of the two multi-path components is reported in Table II on the left. The results confirm that as the ToA grid became denser, the accuracy in the path ToA estimation increases at a cost of a higher computing time. As a tradeoff between accuracy and execution time, we fix the ToA grid granularity for all the approaches to 5×10^{-10} s. The AoA grid granularity is set to 0.5 deg.

Computational complexity and paths resolvability. To properly evaluate and compare the algorithms, both the execution time and the accuracy in the parameter estimation have to be considered. In Table II on the right we report the average execution time for the resolvability of the two multi-path components of the signal for the different approaches. To evaluate the path resolvability, we consider an approach similar to the one adopted in [6]. We fix the maximum tolerable ToA and AoA errors to 5×10^{-9} s and 40 deg respectively

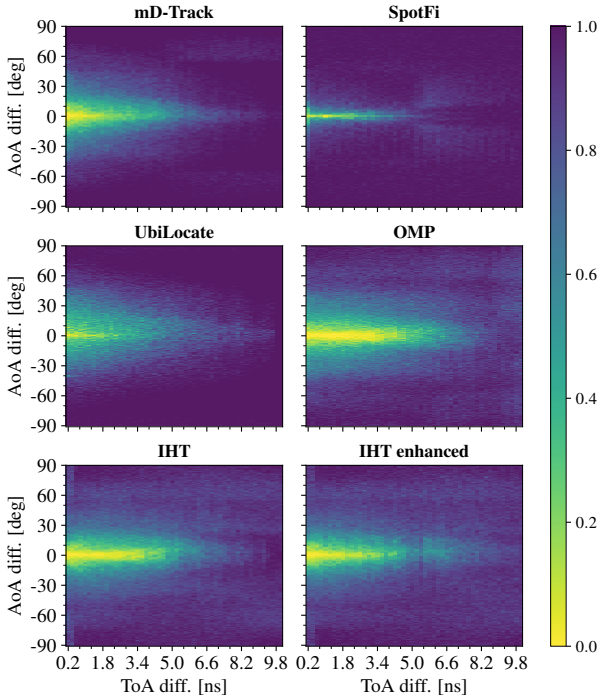

Fig. 3: Path resolvability considering a maximum tolerable ToA and AoA errors of 5×10^{-9} s and 40 deg respectively.

and we analyze the probability of successfully estimating the ToA and AoA parameters of both the paths in the signal. The resolvability index for the six multi-path parameter estimators is reported in Fig. 3, where a value of one means that the paths are completely resolvable while zero means that they are merged into a single path or the parameter estimates are not accurate. The results indicate that, as a tradeoff between execution time and accuracy, the approaches that should be preferred are the three ad-hoc ones (see Section IV).

ToA and AoA estimation errors. In Figs. 4-5 we respectively evaluate the absolute error in the estimation of the ToA and AoA for the first (left plots) and the second (right plots) multi-path components. Previous work in the literature only showed the distribution of the errors through the cumulative density function, without indicating how the errors change based on the ToA and AoA difference between the multi-path components. In our analysis, we found out that such a difference has an impact on the estimation error of both the multi-path components as depicted in Figs. 4-5. Note that the evaluation of the errors can be performed only when the path is recognized, i.e., the errors are smaller than the ToA and AoA tolerances introduced above. The results in Fig. 4 indicate that the ToA error is maximum when the paths are close in the AoA domain. At small ToA differences the error in the first path is close to zero because the two paths cannot be separated (see Fig. 3) and are merged together in a single path that is correctly estimated. The same reasoning applies to the results in Fig. 5 regarding the AoA error. The results indicate that the approach that performs better in the estimation is SpotFi but its execution time is respectively 60 and 30 times the mD-Track and UbiLocate algorithms that can provide sufficient path

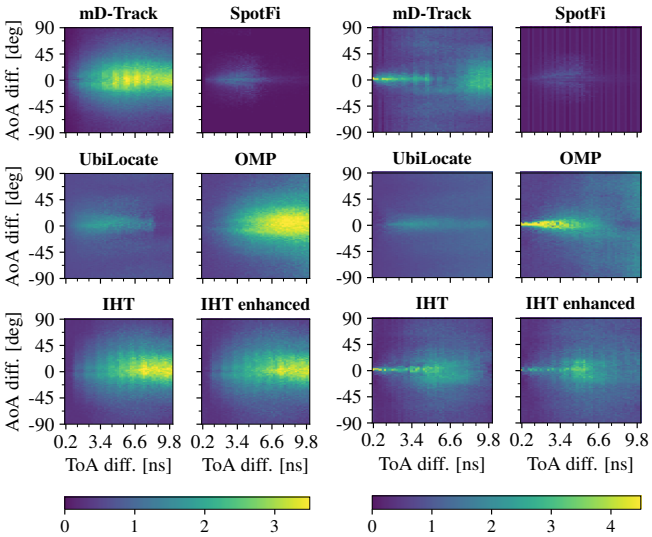

Fig. 4: Error in the estimation of the delay of the first (left) and second (right) paths. The colors indicate the error in ns.

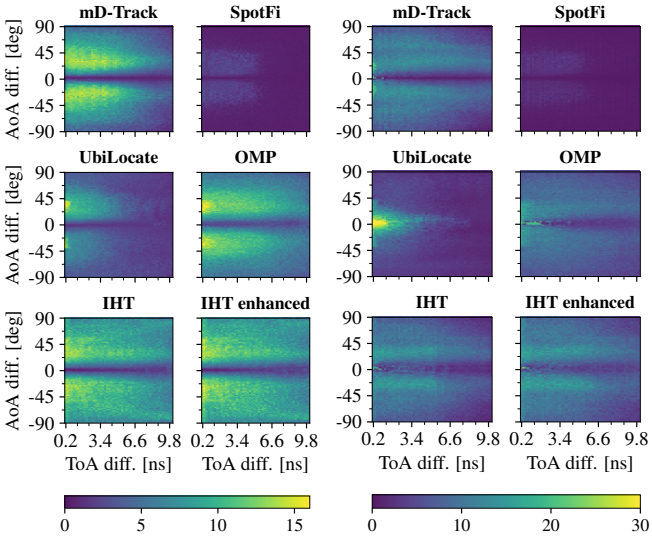

Fig. 5: Error in the estimation of the AoA of the first (left) and second (right) paths. The colors indicate the error in deg.

parameter estimation accuracy for localization as presented in [6], [9]. The compressive sensing-based approaches perform similarly to mD-Track but require higher execution times.

Overall, the results show that multi-path parameter estimation approaches are hardly applicable to vital signs monitoring. Such applications require separating and tracking the contribution of closely spaced paths generated by different body parts, i.e., with almost the same AoA and a ToA difference smaller than $1.6\,\mathrm{ns}$ – corresponding to a space displacement of less than $50\,\mathrm{cm}$. To achieve the required radar-like accuracy, a higher number of antennas and a higher communication bandwidth would be needed. In this respect, the novel IEEE 802.11ay standard provides support for the mmWave spectrum where channels with higher bandwidth can be leveraged for sensing. The new technology is therefore expected to be suitable for multi-path decomposition-based vital signs monitoring. However, commercial devices implementing the new standard are not yet available in the market.

VII. Concluding Remarks

Different super-resolution multi-path parameter estimation strategies have been presented in the literature so far. In this paper, we investigated whether they can be applied to separate the multi-path components for precise human sensing applications. The results show that the estimation errors do not allow properly separating and tracking contributions associated with reflections closely spaced in the ToA/AoA domain like the ones that are generated by the different body parts of a subject. This limits the development of fine-grained Wi-Fi-based human sensing applications, such as vital signs monitoring, on the below $7\,\mathrm{GHz}$ spectrum. Future research avenues include analyzing the performance of the presented multi-path separation algorithms considering higher bandwidth channels (in the mmWave) and devices with more antennas.

Acknowledgment

This work was partially supported by the European Union under the Italian National Recovery and Resilience Plan (NRRP) of NextGenerationEU, partnership on "Telecommunications of the Future" (PE0000001 - program "RESTART").

References

[1] Y. Ma, G. Zhou, and S. Wang, "WiFi Sensing with Channel State Information: A Survey," *ACM Computing Surveys*, vol. 52, no. 3, 2019.

[2] F. Meneghello, C. Chen, C. Cordeiro, and F. Restuccia, "Toward Integrated Sensing and Communications in IEEE 802.11bf Wi-Fi Networks," *IEEE Communications Magazine*, 2023.

[3] C. Chen, H. Song, Q. Li, F. Meneghello, F. Restuccia, and C. Cordeiro, "Wi-Fi Sensing Based on IEEE 802.11bf," *IEEE Communications Magazine*, vol. 61, no. 1, 2022.

[4] Y. Zhang, Y. Zheng, G. Zhang, K. Qian, C. Qian, and Z. Yang, "GaitSense: Towards Ubiquitous Gait-Based Human Identification with Wi-Fi," *ACM Trans. on Sensor Networks*, vol. 18, no. 1, 2021.

[5] F. Meneghello, D. Garlisi, N. D. Fabbro, I. Tinnirello, and M. Rossi, "SHARP: Environment and Person Independent Activity Recognition with Commodity IEEE 802.11 Access Points," *IEEE Trans. on Mobile Computing*, 2022.

[6] Y. Xie, J. Xiong, M. Li, and K. Jamieson, "MD-Track: Leveraging Multi-Dimensionality for Passive Indoor Wi-Fi Tracking," in *Proc. of ACM MobiCom*, 2019.

[7] G. Paterniani, D. Sgreccia, A. Davoli, G. Guerzoni, P. Di Viesti, A. C. Valenti, M. Vitolo, G. M. Vitetta, and G. Boriani, "Radar-Based Monitoring of Vital Signs: A Tutorial Overview," *Proceedings of the IEEE*, vol. 111, no. 3, 2023.

[8] M. Kotaru, K. Joshi, D. Bharadia, and S. Katti, "SpotFi: Decimeter Level Localization Using WiFi," *Proceedings of SIGCOMM Comput. Commun. Rev.*, vol. 45, no. 4, 2015.

[9] A. B. Pizarro, J. P. Beltrán, M. Cominelli, F. Gringoli, and J. Widmer, "Accurate Ubiquitous Localization with Off-the-Shelf IEEE 802.11ac Devices," in *Proc. of ACM MobiSys*, 2021.

[10] A. Goldsmith, *Wireless Communications*. Cambridge Univ. Press, 2005.

[11] M. Vanderveen, C. Papadias, and A. Paulraj, "Joint Angle and Delay Estimation (JADE) for Multipath Signals Arriving at an Antenna Array," *IEEE Communications Letters*, vol. 1, no. 1, 1997.

[12] R. Schmidt, "Multiple Emitter Location and Signal Parameter Estimation," *IEEE Trans. on Antennas and Propagation*, vol. 34, no. 3, 1986.

[13] B. Fleury, M. Tschudin, R. Heddergott, D. Dahlhaus, and K. Ingeman Pedersen, "Channel Parameter Estimation in Mobile Radio Environments using the SAGE Algorithm," *IEEE Journal on Selected Areas in Communications*, vol. 17, no. 3, 1999.

[14] C. R. Berger, Z. Wang, J. Huang, and S. Zhou, "Application of Compressive Sensing to Sparse Channel Estimation," *IEEE Communications Magazine*, vol. 48, no. 11, 2010.

[15] Y. Arjoune, N. Kaabouch, H. El Ghazi, and A. Tamtaoui, "Compressive Sensing: Performance Comparison of Sparse recovery Algorithms," in *Proc. of IEEE CCWC*, 2017.

[16] G. K. Yonina C. Eldar, *Compressed Sensing Theory and Applications*. Cambridge University Press, 2012.